DESIGN OF COMPLEX-VALUED VARIABLE DIGITAL FILTERS AND ITS APPLICATION TO THE REALIZATION OF ARBITRARY SAMPLING RATE CONVERSION FOR COMPLEX SIGNALS

K. M. Tsui, S. C. Chan and K. W. Tse

Department of Electrical and Electronic Engineering,
The University of Hong Kong, Pokfulam Road, Hong Kong.

ABSTRACT

This paper studies the design of complex-valued variable digital filters (CVDFs) and their applications to the efficient arbitrary sample rate conversion for complex signals in software radio receivers. The design of CVDFs using either the minimax or least squares criteria is formulated as a convex optimization problem and solved using the second order cone programming (SOCP) or semidefinite programming (SDP). In addition, linear and convex quadratic inequality constraints can be readily incorporated. Design examples are given to demonstrate the effectiveness of the proposed approach.

I. INTRODUCTION

Variable digital filters (VDFs) [1] are digital filters with controllable spectral characteristics such as variable cutoff frequency, adjustable passband width [2,3], controllable fractional delay [4-7], etc. They are useful in arbitrary sample rate changers [8], digital synchronizers [9], and other applications involving on-line tuning of frequency characteristics. The least squares design criterion is commonly used to design Farrow-based FIR VDFs [2,10,11] because it only involves the solution of a system of linear equation. Linear programming technique [3,7] has also been proposed to design variable digital filters having linear-phase characteristics and minimax design errors. Another method based on semidefinite programming (SDP), which is able to design both linear-phase and low-delay VDFs in either minimax or least square (LS) senses, was briefly discussed in [8]. Most VDFs considered so far have real-valued coefficients. In processing bandpass signals, the baseband signals after frequency down-conversion are usually complex-valued. Therefore, the processing of complex-valued signals using VDFs is of considerable interests, say, in the implementation of software radios or other communication systems.

In this paper, we mainly focus on the complex-valued variable digital filters (CVDFs) design problem, possibly with prescribed number of zeros and peak error constraints in the stopband. Constraints like multiple zeros are desirable in designing sample rate converter in order to suppress the alias components, and the design of wavelet basis. On the other hand, peak error constraints are useful to limit the sidelobe and undesirable peaks in filters with wide unconstrained transition band. Both least squares and minimax design criterion will be considered. As an illustration, we shall formulate these problems as a convex programming problem and solved using second order cone programming (SOCP) [12-14]. Alternatively, another efficient convex optimization tool called semidefinite programming (SDP) [15] can also be used. The constraints for the prescribed number of zeros are derived through a simple relation between the derivatives of the filter response and its ideal counterpart. This yields a set of linear equality constraints, which are imposed to each subfilter coefficients separately so that these constraints can be satisfied over the entire range of the tuning parameter in the Farrow's structure [4]. Within the SOCP (or SDP) framework, these linear equality and convex quadratic inequality constraints such as peak design error can be integrated together in the optimal design of CVDFs with minimax and LS errors satisfying these constraints. Design results show that the proposed method offers an attractive alternative to traditional design methods because of its optimality, generality and flexibility.

As mentioned earlier, one application of VDFs is to realize SRC, which is an essential component in software radio receivers [16]. The basic idea of a VDF-based SRC is to provide variable fractional delay in the passband and additional attenuation in the stopband. Therefore, arbitrary sampling rate conversion can be achieved by tuning the control parameter in the Farrow's structure. In this work, the approach in [8] is extended to complex-valued input signals possibly with an asymmetric magnitude and phase characteristics. The proposed CVDF, which has asymmetry frequency response, thus offers greater freedom and flexibility for processing these signals.

The paper is organized as follows: Section II is devoted to the problem formulation of CVDFs using either minimax or LS design criteria. Methods for deriving the prescribed number of zeros and peak design error constraints will also be introduced. Design examples, including the design of SRC for complex-valued signals, are given in Section III to demonstrate the effectiveness of the proposed approach. Finally, conclusion is drawn in Section IV.

II. PROBLEM FORMULATION

A.— Complex-valued variable digital filter (VDF) design

In a VDF [2], the desired response $H_d(\omega,\phi)$ is a function of a spectral parameter ϕ (also known as tuning or control parameters). The spectral characteristics of a VDF can therefore be continuously varied by changing ϕ. The impulse response of the VDF under consideration is assumed to be a linear combination of a polynomial basis function of the spectral parameter ϕ and subfilter coefficients $h_l(n)$, and it is given by:

$$h(n,\phi)=\sum_{l=0}^{L-1}h_l(n)\cdot\phi^l\,, \tag{2-1}$$

where ϕ is assumed to vary linearly over a finite interval. The z-transform of the polynomial-based VDF is then given by:

$$H(z,\phi)=\sum_{l=0}^{L-1}\left[\sum_{n=0}^{N-1}h_l(n)z^{-n}\right]\cdot\phi^l=\sum_{l=0}^{L-1}H_l(z)\cdot\phi^l\,, \tag{2-2}$$

where $H_l(z)=\sum_{n=0}^{N-1}h_l(n)z^{-n}$ is the l-th FIR subfilter. (2-2) suggests a very useful structure for implementing VDF called the Farrow's structure, which is shown in figure 1. Suppose that the impulse response of the l-th complex subfilter is given by $h_l(n)=h_{R,l}(n)+jh_{I,l}(n)$ for $n=0,1,\ldots,N-1$. By defining

$$\begin{aligned}
&\boldsymbol{a}=[\boldsymbol{h}_{R,0}{}^T,\ldots,\boldsymbol{h}_{R,L-1}{}^T,\boldsymbol{h}_{I,0}{}^T,\ldots,\boldsymbol{h}_{I,L-1}{}^T]^T,\\
&\boldsymbol{h}_{R,l}=[h_{R,l}(0),\ldots,h_{R,l}(N-1)]^T \text{ for } l=0,1,\ldots,L-1,\\
&\boldsymbol{h}_{I,l}=[h_{I,l}(0),\ldots,h_{I,l}(N-1)]^T \text{ for } l=0,1,\ldots,L-1,\\
&\boldsymbol{c}_2(\omega,\phi)=[\boldsymbol{c}_1(\omega,\phi)^T,\boldsymbol{s}_1(\omega,\phi)^T]^T,\\
&\boldsymbol{s}_2(\omega,\phi)=[\boldsymbol{s}_1(\omega,\phi)^T,-\boldsymbol{c}_1(\omega,\phi)^T]^T,\\
&\boldsymbol{c}_1(\omega,\phi)=[\boldsymbol{c}(\omega)^T,\phi^1\cdot\boldsymbol{c}(\omega)^T,\ldots,\phi^{L-1}\cdot\boldsymbol{c}(\omega)^T]^T,\\
&\boldsymbol{s}_1(\omega,\phi)=[\boldsymbol{s}(\omega)^T,\phi^1\cdot\boldsymbol{s}(\omega)^T,\ldots,\phi^{L-1}\cdot\boldsymbol{s}(\omega)^T]^T,\\
&\boldsymbol{c}(\omega)=[1,\cos\omega\ldots,\cos((N-1)\omega)]^T \text{ and}\\
&\boldsymbol{s}(\omega)=[0,\sin\omega\ldots,\sin((N-1)\omega)]^T,
\end{aligned} \tag{2-3}$$

(2-2) can be written as:

$$H(e^{j\omega},\phi)=\boldsymbol{a}^T\{\boldsymbol{c}_2(\omega,\phi)-j\boldsymbol{s}_2(\omega,\phi)\}. \quad (2\text{-}4)$$

We want to approximate the desired response $H_d(z,\phi)$ by $H(z,\phi)$ in the minimax sense. That is:

$$\min_{\boldsymbol{a}}\max_{\Omega}\{W(\omega,\phi)\left|H(e^{j\omega},\phi)-H_d(\omega,\phi)\right|\},\ (\omega,\phi)\in\Omega, \quad (2\text{-}5)$$

where $W(\omega,\phi)$ is a positive weighting function, and Ω is the (frequency, tuning range) of interest. Let $H_{R\_d}(\omega,\phi)$ and $H_{I\_d}(\omega,\phi)$ be the real and imaginary parts of $H_d(\omega,\phi)$, the minimization problem in (2-5) can be reformulated as:

$$\min_{\boldsymbol{a}}\ \delta$$
$$\text{subject to } \delta-[\alpha_R^2(\omega,\phi)+\alpha_I^2(\omega,\phi)]^{1/2}\ge 0,\ (\omega,\phi)\in\Omega, \quad (2\text{-}6)$$

$$\text{where}\quad \begin{aligned}\alpha_R(\omega,\phi)&=W(\omega,\phi)\cdot[\boldsymbol{a}^T\boldsymbol{c}_2(\omega,\phi)-H_{R\_d}(\omega,\phi)],\\ \alpha_I(\omega,\phi)&=W(\omega,\phi)\cdot[\boldsymbol{a}^T\boldsymbol{s}_2(\omega,\phi)+H_{I\_d}(\omega,\phi)].\end{aligned} \quad (2\text{-}7)$$

Digitizing the frequency variable ω and control parameter ϕ over a dense set of frequencies $\{\omega_i, 1\le i\le K_1\}$ and control parameters $\{\phi_k, 1\le k\le K_2\}$ in the range of interests, the constraints in (2-6) becomes:

$$\delta-[\alpha_R^2(\omega_i,\phi_k)+\alpha_I^2(\omega_i,\phi_k)]^{1/2}\ge 0, \quad (2\text{-}8)$$

Moreover, by defining the augmented variable $\boldsymbol{x}=[\delta\quad \boldsymbol{a}^T]^T$, (2-6) can be cast to the standard SOCP problem as follows:

$$\min_{\boldsymbol{x}}\ \boldsymbol{c}^T\boldsymbol{x}\quad \text{subject to } \boldsymbol{c}^T\boldsymbol{x}\ge\left\|\boldsymbol{F}_{i,k}\boldsymbol{x}-\boldsymbol{g}_{i,k}\right\|_2, \quad (2\text{-}9)$$

$$\boldsymbol{c}=[1,0,\ldots 0]^T,$$

$$\text{where}\quad \boldsymbol{F}_{i,k}=W(\omega_i,\phi_k)\cdot\begin{bmatrix}0 & \boldsymbol{c}_2(\omega_i,\phi_k)^T\\ 0 & \boldsymbol{s}_2(\omega_i,\phi_k)^T\end{bmatrix}\ \text{and} \quad (2\text{-}10)$$

$$\boldsymbol{g}_{i,k}=W(\omega_i,\phi_k)\cdot[H_{R\_d}(\omega_i,\phi_k)\quad -H_{I\_d}(\omega_i,\phi_k)]^T$$

Alternatively, (2-5) can be formulated as a SDP problem [8,15], which might provide more flexibility but requires a longer design time. For simplicity, only the SOCP formulation is considered below. Instead of using the minimax criterion, the least squares stopband attenuation:

$$E_{LS}=\int_{\Omega}W(\omega,\phi)\cdot\left|H(e^{j\omega},\phi)-H_d(e^{j\omega},\phi)\right|^2 d\omega d\phi, \quad (2\text{-}11)$$

can be minimized. The advantage of minimizing E_{LS} is that it can be written as a quadratic function of $\boldsymbol{a}$:

$$\min_{\boldsymbol{a}}\ \boldsymbol{a}^T\boldsymbol{Q}\boldsymbol{a}-2\boldsymbol{a}^T\boldsymbol{p}+k, \quad (2\text{-}12)$$

where $\boldsymbol{Q}=\int_{\Omega}W(\omega,\phi)\cdot[\boldsymbol{c}_2(\omega,\phi)\boldsymbol{c}_2(\omega,\phi)^T+\boldsymbol{s}_2(\omega,\phi)\boldsymbol{s}_2(\omega,\phi)^T]d\omega d\phi$

$\boldsymbol{p}=\int_{\Omega}W(\omega,\phi)[\boldsymbol{c}_2(\omega,\phi)H_{R\_d}(\omega,\phi)+\boldsymbol{s}_2(\omega,\phi)H_{I\_d}(\omega,\phi)]d\omega d\phi$,

and $k=\int_{\Omega}W(\omega,\phi)\left|H_d(\omega,\phi)\right|^2 d\omega d\phi$. The optimal LS solution is given by $\boldsymbol{a}_{LS}=\boldsymbol{Q}^{-1}\boldsymbol{p}$. To formulate (2-12) as a SOCP problem, define that $\overline{\boldsymbol{Q}}=[\boldsymbol{O}_N\quad \boldsymbol{Q}^{1/2}]$, $\overline{\boldsymbol{p}}=\boldsymbol{Q}^{-1/2}\boldsymbol{p}$ and $\overline{k}=\boldsymbol{p}^T\boldsymbol{Q}^{-1}\boldsymbol{p}-k$, one can reformulate it as follows:

$$\min_{\boldsymbol{x}}\ \boldsymbol{c}^T\boldsymbol{x}\quad \text{subject to } \boldsymbol{c}^T\boldsymbol{x}-\overline{k}\ge\left\|\overline{\boldsymbol{Q}}\boldsymbol{x}-\overline{\boldsymbol{p}}\right\|_2. \quad (2\text{-}13)$$

where $\boldsymbol{O}_D$ is a D row zero vector. The advantage of formulating the objective function as a convex problem such as SOCP or SDP is that the resulting problem is convex and the optimal solution, if it exists, can be found. In addition, other linear equalities or convex quadratic constraints can easily be incorporated, as we shall illustrate in later sections.

B. — Imposing multiple zeros in the stopband

As mentioned earlier, it is often required to impose certain constraints on the frequency characteristics when designing digital filters. One commonly encountered constraint is prescribed number of zeros in the stopband, which are desirable in designing sample rate converter in order to suppress the alias components. The following relation between the derivatives of the design response and its ideal counterparts is employed:

$$\left.\frac{d^v}{d\omega^v}H(e^{j\omega},\phi)\right|_{\omega=\hat{\omega}_s}=0,\ v=0,1,\ldots,V_{\hat{\omega}_s}-1. \quad (2\text{-}14)$$

Substituting (2-14) into (2-2), we have:

$$\sum_{n=0}^{N-1}\sum_{l=0}^{L-1}n^v\cdot h_l(n)\cdot\phi^l e^{-j\hat{\omega}_s n}=0,\ v=0,1,\ldots,V_{\hat{\omega}_s}-1. \quad (2\text{-}15)$$

In order to satisfy (2-15) over the entire range of the tuning parameter ϕ, the following constraints are imposed to each subfilter:

$$\sum_{n=0}^{N-1}n^v\cdot h_l(n)\cdot e^{-j\hat{\omega}_s n}=0,\ v=0,1,\ldots,V_{\hat{\omega}_s}-1\ \text{and}\ l=0,1,\ldots,L-1. \quad (2\text{-}16)$$

Equating the real and imaginary parts of (2-16), one gets:

$$\sum_{n=0}^{N-1}n^v\cdot h_{R,l}(n)\cdot\cos(\hat{\omega}_s n)=0,\ \text{or}\ \boldsymbol{Ch}_{R,l}=\boldsymbol{O}_{V_{\hat{\omega}_s}} \quad (2\text{-}17a)$$

$$\sum_{n=0}^{N-1}n^v\cdot h_{R,l}(n)\cdot\sin(\hat{\omega}_s n)=0,\ \text{or}\ \boldsymbol{Sh}_{R,l}=\boldsymbol{O}_{V_{\hat{\omega}_s}} \quad (2\text{-}17b)$$

$$\sum_{n=0}^{N-1}n^v\cdot h_{I,l}(n)\cdot\cos(\hat{\omega}_s n)=0,\ \text{or}\ \boldsymbol{Ch}_{I,l}=\boldsymbol{O}_{V_{\hat{\omega}_s}} \quad (2\text{-}17c)$$

$$\sum_{n=0}^{N-1}n^v\cdot h_{I,l}(n)\cdot\sin(\hat{\omega}_s n)=0,\ \text{or}\ \boldsymbol{Sh}_{I,l}=\boldsymbol{O}_{V_{\hat{\omega}_s}} \quad (2\text{-}17d)$$

where $[\boldsymbol{C}]_{v,n}=n^v\cos(\hat{\omega}_s n)$ and $[\boldsymbol{S}]_{v,n}=n^v\sin(\hat{\omega}_s n)$, for $v=0,1,\ldots,V_{\hat{\omega}_s}-1$ and $l=0,1,\ldots,L-1$. Here, $[A]_{m,n}$ denotes the $(m,n)-th$ entry of matrix $\boldsymbol{A}$. It should be noted that some of the constraints in (2-17) can be eliminated when $\hat{\omega}_s=d\pi/4$; $d=0,\pm1,\ldots,\pm4$. Moreover, the above constraints can be imposed at more than one frequency point as long as the total number of linear equality constraints does not exceed the filter length N. Otherwise, there will be insufficient freedom in the filter coefficients to satisfy all these constraints. The constraints in (2-17) can also be combined to form the following matrix representation for $\boldsymbol{h}_{R,l}$ and $\boldsymbol{h}_{I,l}$, respectively:

$$\boldsymbol{A}_{\beta,l}\boldsymbol{h}_{\beta,l}=\boldsymbol{O}_{2V_{\hat{\omega}_s}},\ l=0,1,\ldots,L-1, \quad (2\text{-}18)$$

where $\boldsymbol{A}_{\beta,l}=[\boldsymbol{C}^T\quad \boldsymbol{S}^T]^T$.

β represents either R or I. To incorporate these constraints into the design problem, we combine (2-18) as follows:

$$\boldsymbol{A}\boldsymbol{a}=\boldsymbol{O}_{4LV_{\hat{\omega}_s}}, \quad (2\text{-}19)$$

where $\boldsymbol{A}=diag\{\boldsymbol{A}_{R,0},\ldots,\boldsymbol{A}_{R,L-1},\boldsymbol{A}_{I,0},\ldots,\boldsymbol{A}_{I,L-1}\}$.

The minimization in (2-9) and (2-13) can be solved subject to these linear equality constraints using SOCP.

C. —Peak error and convex quadratic constraints

To avoid excessive sidelobe of the LS solution, additional peak constraints can be imposed to the stopband. Let δ_p be the peak ripple to be imposed in a frequency band $\omega\in[\omega_1,\omega_2]$ (a collection of frequency bands is also feasible), then the peak error constraint can be written as:

$$\left|H(e^{j\omega},\phi)\right|\le\delta_p,\ \omega\in[\omega_1,\omega_2],\ (\omega,\phi)\in\Omega. \quad (2\text{-}20)$$

Similar to the minimax formulation, (2-20) can be rewritten as:

$$\delta_p\ge\left\|\boldsymbol{R}\boldsymbol{x}\right\|_2, \quad (2\text{-}21)$$

$$\text{where}\quad \boldsymbol{R}=\begin{bmatrix}0 & \boldsymbol{c}_2(\omega,\phi)^t\\ 0 & \boldsymbol{s}_2(\omega,\phi)^t\end{bmatrix}.$$

After digitizing ω and ϕ over the range of interest, the resulting constraints on the peak ripples can be augmented to the existing constraints in (2-9) and (2-13) for the minimax and LS criterion respectively.

III. DESIGN OF COMPLEX SRC

A. — Complex-valued variable digital filter (CVDF) design

The design of programmable SRCs with arbitrary conversion factors was studied in detail by Ramstad [17]. In general, there are two approaches to implement a SRC with different tradeoff between the sampling rate and the hardware complexity. One is to up-sample the input signal by a factor of L, i.e. inserting $L-1$ zeros between successive time samples. This creates $L-1$ images in the frequency domain, which are then removed by an interpolated filter. If L is sufficiently large, further interpolation with an irrational downsampling ratio can be achieved simply by a low-order interpolator, which is controlled by a tuning parameter and is able to provide rather accurate fractional delays up to a certain frequency, say 0.1π. After which, both the amplitude and phase responses deviate considerably from an ideal fractional-delay digital filter (FDDF) [4,5]. Alternatively, these functions can also be implemented using a VDF [2,11] with a control parameter ϕ. For modest downsampling ratios, the VDF-based SRC is more efficient than the former approach because its coefficients can be jointly optimized to fulfill the given spectral and fractional-delay specifications [8]. For larger sampling conversion factors, a combination of these approaches can be used.

For complex-valued signals, similar arguments still hold, except that its frequency spectrum is not symmetric about $\omega=0$. To accommodate this asymmetric spectrum, we assume that the filter coefficients are complex quantities, which can be optimized using the proposed design method. The complex VDF-based SRC has the following ideal frequency response:

$$H_d(e^{j\omega},\phi)=\begin{cases}e^{-j\omega\tau(\phi)}, & \Omega_p\in[\omega_{p1},\omega_{p2}]\\ 0, & \Omega_s\in[-\pi,\omega_{s1}]\cap[\omega_{s2},\pi]\end{cases}, \quad (3\text{-}1)$$

where $\tau(\phi)=(N-1)/2-D+\phi$ is the group delay of the VDF-based SRC; D is the delay reduction parameter; Ω_p and Ω_s are the frequency of interest at the passband and stopband respectively; ω_{p1} and ω_{p2} (ω_{s1} and ω_{s2}) are the passband (stopband) cutoff frequencies. Without loss of generality, we assume that $-\pi<\omega_{p1}, \omega_{s1}<0$, and $0<\omega_{p2},\omega_{s2}<\pi$. In the passband of the CVDF, it behaves like a tunable fractional delay digital filter and the tuning parameter ϕ is used to provide the required arbitrary fractional delays. In the stopband, it helps to attenuate the undesirable frequency components.

Design Example 1

We now consider the design of complex-valued VDF-based SRCs using the proposed method. All the design problems were solved by the *SeDuMi* Matlab Toolbox [18] on a Pentium 4 PC. The specifications are: $N=17$, $L=5$, $D=0$, $\omega_{p1}=-0.2\pi$, $\omega_{p2}=0.4\pi$, $\omega_{s1}=-0.7\pi$, $\omega_{s2}=0.8\pi$, $K_1=100$, $\phi\in[-0.5,0.5]$ and $K_2=50$. Two zeros at $\omega=\pi$ are enforced in our CVDFs: i.e. $V_\pi=2$. The frequency and group delay responses of the CVDF using minimax criterion with ϕ = 0, 0.1, 0.2, 0.3, 0.4 and 0.5 are shown in figures 2a and 2b, respectively. The corresponding passband deviation and stopband attenuation are respectively 0.0076 dB and 60.7465 dB. The computational time is about 15.9761 minutes. Alternatively, we can solve the above problem using LS criterion. The design time is greatly reduced to 0.0297 minutes. To further reduce the sidelode, the peak stopband constraint is imposed as in (2-20) and (2-21). Figures 2c and 2d show its frequency and group delay responses so obtained. In exchange for slightly lower performance at the unconstrained frequency bands, the maximum stopband attenuation is now increased to 60 dB, compared to 54.6477 dB for the LS design. The time required is longer than the LS approach, but much lower than that using the minimax approach. Table 1 summarizes the design results in this example. It should be noted that when solving minimax criterion, the design time is rather long since the number of constraints and variables increases exponentially with the dimension of the problem. Same difficulties would be encountered by 2D digital filter design or even 2D VDF design. As a comparison, SDP method is also implemented, and it is noticed from table 1 that much longer computational time is required in the SDP approach with a similar performance. Due to page limitation, details of the SDP formulation and the corresponding design results are omitted for simplicity.

B. — Complex-valued Anti-aliasing lowpass filters

In [8], the multistage decimator is inserted prior to the VDF-based SRC, which is designed to support a downsampling ratio of $M_{SRC}\in(1,2)$, so as to provide larger decimation ratio to the input signals. In order to remove the residue interference, the output of the SRC is fed to an additional anti-aliasing lowpass filter, denoted by LPF_f. The overall structure is depicted in figure 3a. It can be seen that the overall downsampling ratio M^* is then given by:

$$M^*=M_{SRC}\cdot 2^k, \quad (3\text{-}2)$$

where k is the number of the remaining 2-to-1 decimators to be selected.

Design Example 2

As an illustration, a two-stage decimator, as shown in figure 3b, is employed so that M^* lies between 2 and 16. The target passband deviation and stopband attenuation of the overall SRC are respectively 0.2dB and 60 dB. Also, we assume that the largest possible spectrum of the complex-valued input signal occupy the frequency band, lying in the interval $[-0.3\pi,0.5\pi]$. Because the magnitude spectrum is asymmetric around the origin (such as in VSB modulation), it might be better to employ a complex SRC to limit unnecessary noise or interference, instead of using a real-valued SRC with bandwidth from $[-0.5\pi,0.5\pi]$. The resulting complex-valued anti-aliasing lowpass filters are designed using the proposed SOCP formulation, simply by setting $L=1$, $\phi=0$ and $K_2=1$. All these anti-aliasing lowpass filters are designed in minimax sense. The specifications and performances of the anti-aliasing lowpass filters are summarized in Table 2. Their frequency responses are shown in figure 4. Together with the CVDF as designed in previous example, the overall SRC gives a passband deviation of 0.194 dB and stopband attenuation of 60.13 dB, as shown in table 3. The frequency responses of the resulting complex-valued SRC with different operating ranges are shown in figure 5.

V. CONCLUSION

A method for designing complex-valued VDFs (CVDFs) with prescribed flatness and peak error constraints using convex problem has been presented. Optimal minimax and LS design are considered. Design examples using sample rate converters for complex signals in software radio receivers are given to illustrate the effectiveness of the proposed approach. It shows that the proposed method offers more flexibility and good performance in incorporating a wide variety of constraints than conventional methods.

REFERENCES

[1] R. Zarour and M. M. Fahmy, "A design technique for variable digital filters," *IEEE Trans. Circuits Syst. II*, vol. 36, pp. 1473-1478, Nov. 1989.

[2] K. S. Pun, S. C. Chan, K. S. Yeung and K. L. Ho, "On the Design of FIR and IIR Digital Filters with Variable Frequency Characteristics," *IEEE Trans. Circuits Syst. II*, vol. 49, no. 11, pp. 689-703, Nov, 2002.

[3] P. Lowenborg and H. Johansson, "Linear Programming Design of Linear-phase FIR Filters with Variable Bandwidth," in *Proc. ISCAS'2003*, vol. 3, pp. 554-557, May 2003.

[4] C. W. Farrow, "A Continuously Variable Digital Delay Element," in *Proc. ISCAS*, vol. 3, pp. 2641-2645, 1988.

[5] J. Vesma and T. Saramaki, "Design and properties of polynomial-based fractional delay filters," in *Proc. of ISCAS 2000*, pp.104-107.

[6] T. I. Laakso, V. Valimaki, M. Karjalainen and U. K. Laine, "Splitting the unit delay, tools for fractional delay filter design," *IEEE Signal Processing Mag.*, pp.30-60, Jan. 1996.

[7] H. Johansson and P. Lowenborg, "On the Design of Adjustable Fractional Delay FIR Filters," *IEEE Trans. Circuits Syst. II*, vol. 50, no. 4, pp. 164-169, April 2003.

[8] S. C. Chan and K. S. Yeung, "On the application of variable digital filters (VDF) to the realization of software radio receivers," in *Proc. ISCAS'2003*, vol. 3, pp. 562-565, May 2003.

[9] L. Erup, F. M. Gardner and R. A. Harris, "Interpolation in digital modems. II. Implementation and performance," *IEEE Trans. Commun.*, vol. 41, pp. 998-1008, Jun. 1993.

[10] A. Tarczynski, G. D. Cain, E. Hermanowicz and M. Rojewski, "WLS design of variable frequency response FIR filters," in *Proc. ISCAS 1997*, vol. 4, pp. 2244-2247, 1997.

[11] W. S. Lu and T. B. Deng, "An Improved Weighted Least-squares Design for Variable Fractional Delay FIR Filters," *IEEE Trans. Circuits Syst II*, vol. 9, pp. 689-685, Sept.1997.

[12] M. S. Lobo, L. Vandenberghe, S. Boye and H. Lebret, "Applications of second-order cone programming", *Linear Algerba Application*, vol. 248, pp. 193-228, Nov. 1998.

[13] W. S. Lu and T. Hinamoto, "Optimal design of FIR frequency-response-masking filters using second-order cone programming", in *Proc. ISCAS'2003*, vol. 3, pp. 878-881, May 2003.

[14] J. O. Coleman and D. P. Scholnik, "Design of non-linear phase FIR filters with second-order cone programming", in *Proc. MWSCAS 1999*, vol. 1, pp. 409-412, Aug. 1999.

[15] H. Wolkowicz, R. Saigal and L. Vandenberge, "Handbook of Semidefinite Programming: theory, algorithms, and applications", *Kluwer Academic Publishers*, 2000.

[16] T. Hentschel and G. Fettweis, "Sample rate conversion for software radio," *IEEE Commn. Mag.*, pp. 142-150, Aug. 2000.

[17] T. A. Ramstad, "Digital methods for conversion between arbitrary sampling frequencies," *IEEE Trans. ASSP-32*, pp. 577-591, 1984.

[18] J. F. Sturm, "Using SeDuMi 1.02, a MATLAB toolbox for optimization over symmetric cones," *Optim. Meth. Softw.*, vol. 11-12, pp. 625-653, 1999.

Design criteria	Minimax	LS	LS
V_π	2	2	2
Peak stopband	N/A	N/A	-60dB
Passband deviation (dB)	0.0076	0.0100	0.0143
Stopband attenuation (dB)	60.7465	54.6477	60
Group delay error (samples)	0.0232	0.0235	0.0246
SOCP design time (min)	15.9761	0.0297	4.7576
SDP design time (min)	176.0303	0.8596	25.3816

Table 1. Design results of the complex-valued variable digital filters.

	LPF#1	LPF#2	LPF$_f$
(ω_{p1} , ω_{p2})	(-0.05 π , 0.1 π)	(-0.1 π , 0.2 π)	(-0.2 π , 0.4 π)
(ω_{s1} , ω_{s2})	(-0.85 π , 0.9 π)	(-0.7 π , 0.8 π)	(-0.4 π , 0.6 π)
Filter length N	7	12	26
V_π	1	1	1
Passband deviation (dB)	6.02×10^{-3}	3.21×10^{-3}	7.26×10^{-3}
Stopband attenuation (dB)	63.21	68.04	61.66

Table 2. Specifications and design results of the anti-aliasing lowpass filters.

Range of M^*	Passband deviation	Stopband attenuation
$2\le M^*\le4$	0.0143 dB	60.13 dB
$4\le M^*\le8$	0.0173 dB	60.13 dB
$8\le M^*\le16$	0.0194 dB	60.13 dB

Table 3. Performances of the SRC for different overall downsampling ratio M^* .

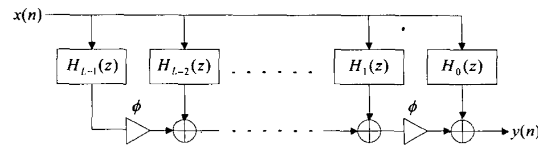
Figure 1: General structure of FIR VDF.

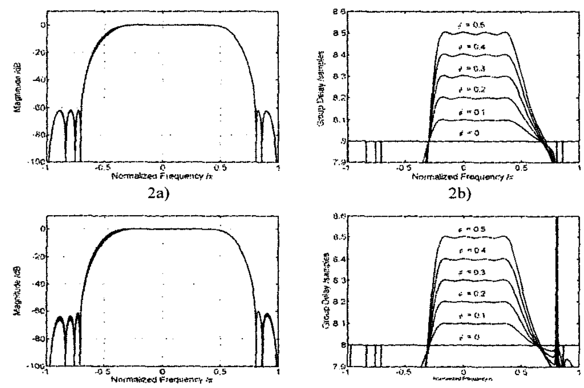
2a) 2b) 2c) 2d)

Figure 2: a) and c) Frequency responses, b) and d) The corresponding group delays of the VDF-based SRC with $\phi=\{0,0.1,0.2,0.3,0.4,0.5\}$ using minimax and LS criteria, respectively.

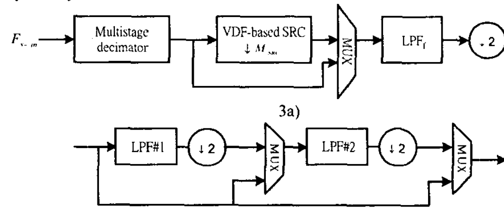
3a) 3b)

Figure 3: a) Overall structure of SRC b) Multistage decimator

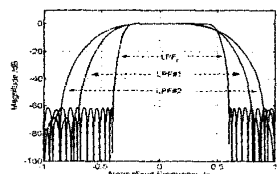
Figure 4: Frequency responses of LPF#1, LPF#2 and LPF$_f$.

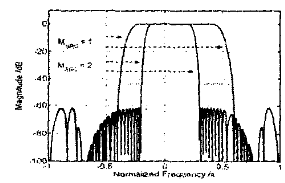
5a)

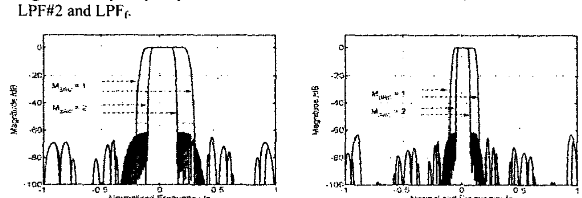
5b) 5c)

Figure 5: Frequency responses of the overall SRC with a) $2\le M^*\le4$, i.e. cascading the LPF$_f$ and CVDF with $M_{SRC}\in(1,2)$, b) $4\le M^*\le8$, i.e. cascading the LPF#2, LPF$_f$ and the CVDF with $M_{SRC}\in(1,2)$, and c) $8\le M^*\le16$, i.e. cascading the LPF#1, LPF#2, LPF$_f$ and the CVDF with $M_{SRC}\in(1,2)$.